Site Characterization for Carbon Storage

NATIONAL ENERGY TECHNOLOGY LABORATORY

Introduction

Carbon Capture, Utilization and Sequestration (CCUS)

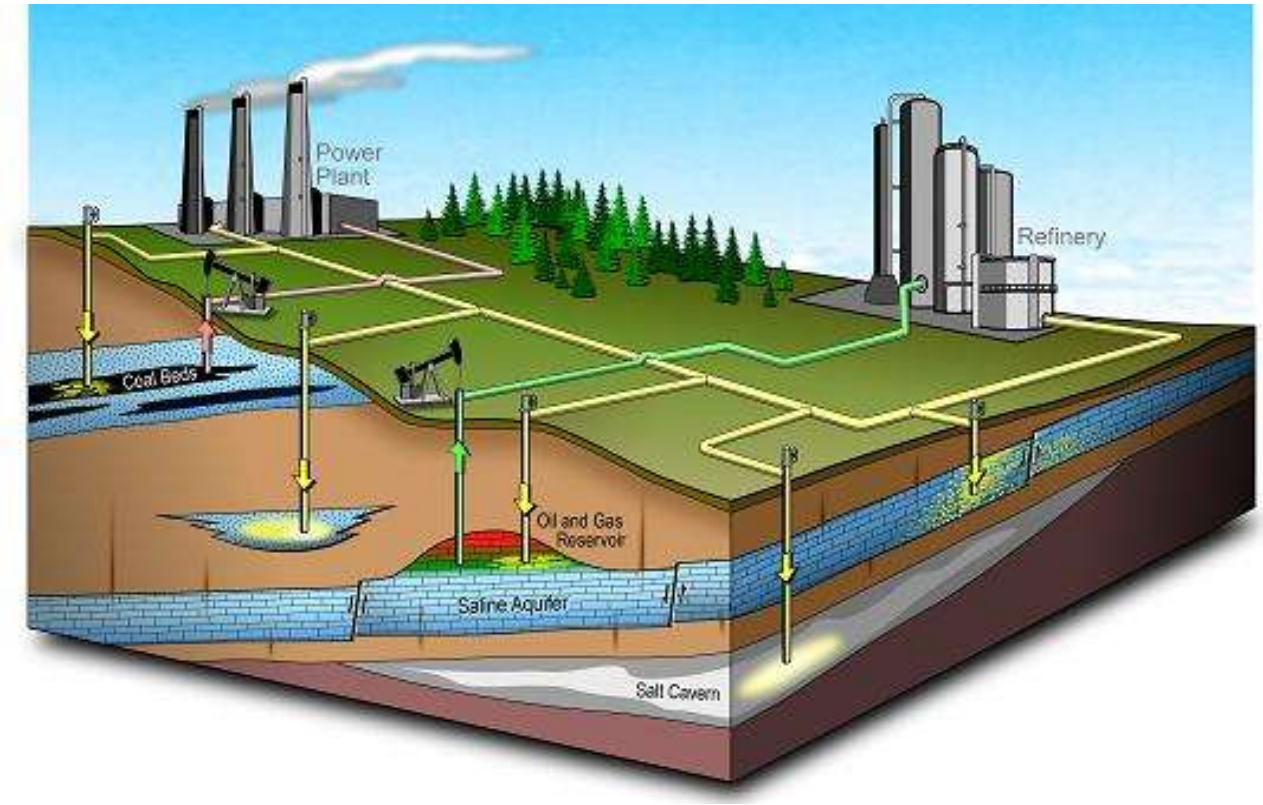

Introduction

Geologic Sink Capacity Estimates--*Adequate Storage Projected*

U.S. emissions ~ 6 Gt CO_2 / yr, all sources

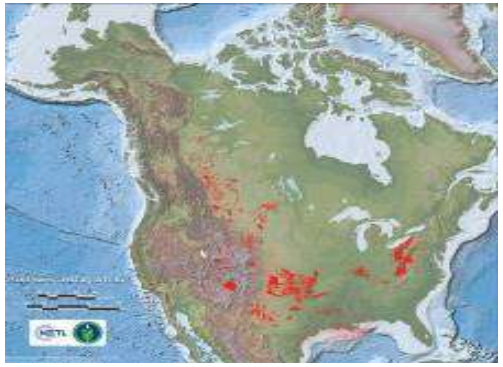

Oil and Gas Fields

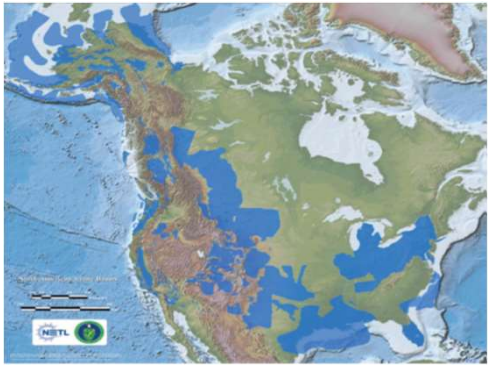

Saline Formations

4,674 stationary sources identified

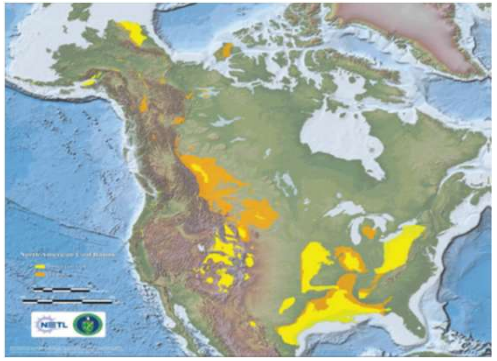

Unmineable Coal Seams

Conservative resource assessment

Estimated North American CO_2 Storage Potential (Gigatonnes)

Sink Type	Low	High
Oil and Gas Fields	140	140
Saline Formations	3,300	12,600
Unmineable Coal Seams	160	180

Hundreds of years storage potential

Is geologic storage of CO_2 conceptually simple ?

- CO_2 is compressed to supercritical conditions and injected into voids (pores) in rock that are originally occupied by water, oil, or gas.
- CO_2 must be trapped (e.g., by low permeability units, dissolution into brine, residual trapping, conversion to solid carbonates, or sorption).

Concerns

- Injection of CO_2 into deep saline formations may cause a range of coupled thermal, hydrodynamic, mechanical and chemical process (White et al., 2003).
- The changes could cause the dissolution of mineral and/or precipitation of secondary mineral phases, and thus change the morphology, porosity, permeability of hosting rocks (Luquot and Gouze 2009., H. Shao et al., 2010, Liu et al., 2012, Soong et al., 2014, 2016, Zhang et al., 2015, 2016)
- Therefore, understanding the interactions between minerals and CO_2/brine is critical to achieve better prediction of the short/long storage of CO_2.
- What would be the long term impacts of CO_2 on storage formation and seals (30 years or longer) ?

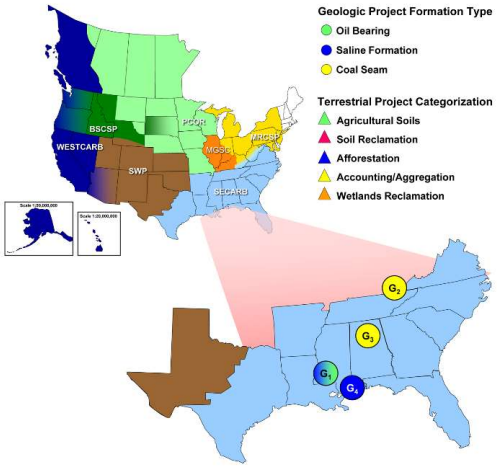

NATIONAL ENERGY TECHNOLOGY LABORATORY

Escatawpa, Mississippi
Plant Daniel Site (Saline) : Validation Phase
Saline formation :(Massive Sand, Lower Tuscaloosa)
CO_2 injected 2,740 metric tons

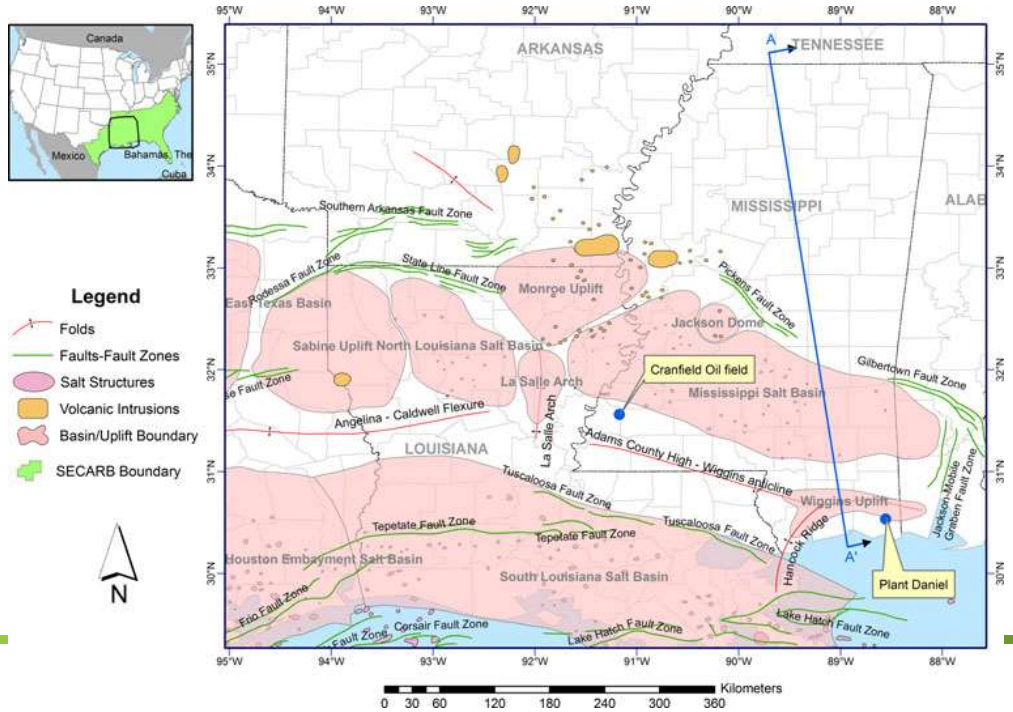

Lower Tuscaloosa Formation

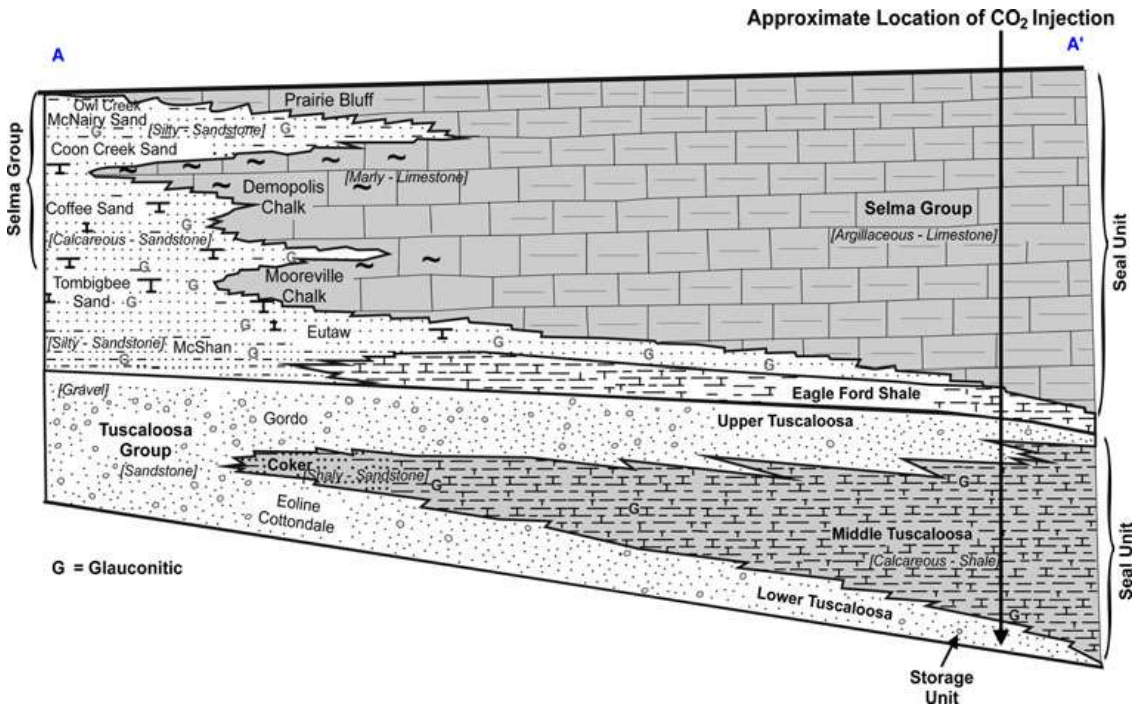

System	Series	Stratigraphic Unit	Sub-Units	Hydrology
Tertiary	Miocene	Misc. Miocene Units	Pascagoula Fm.	Freshwater Aquifers
			Hattiesburg Fm.	
			Catahoula Fm.	
	Oligocene	Vicksburg		Saline Reservoir
			Red Bluff Fm.	Minor confining unit
	Eocene	Jackson		Saline Reservoir
		Claiborne		Saline Reservoir
		Wilcox		Saline Reservoir
	Paleocene	Midway Shale		Confining unit
Cretaceous	Upper	Selma Chalk	Navarro Fm.	Confining unit
			Taylor Fm.	
		Eutaw	Austin Fm.	Confining unit
			Eagle Ford Fm.	Saline Reservoir
		Tuscaloosa Group	Upper Tusc.	Minor Reservoir
			Marine Tusc.	Confining unit
			Lower Tusc.	Saline Reservoir
	Lower	Washita-Fredricksburg	Dantzler Fm.	Saline Reservoir
			"Limestone Unit"	

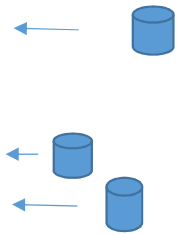

Samples from Escatawpa, Mississippi

	Lower Tuscaloosa Massive Sand	Marine Shale	Selma Chalk
Depth (m)	2611	2418	1894
Porosity	26.5	8.65	12.4
Quartz	77	60	3
Chlorite	6	9	3
Kaolinite	3	5	2
Illite	3	5	2
K-feldspar	1	2	~
Plagioclase	7	12	~
Calcite	1	5	90
Pyrite	2	2	~

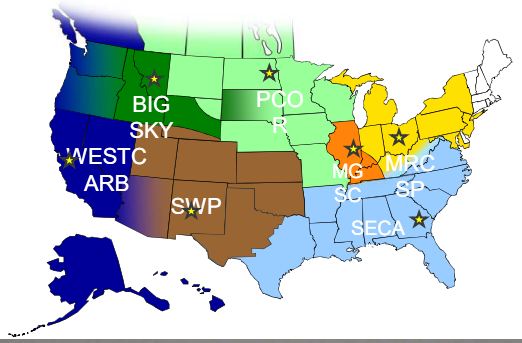

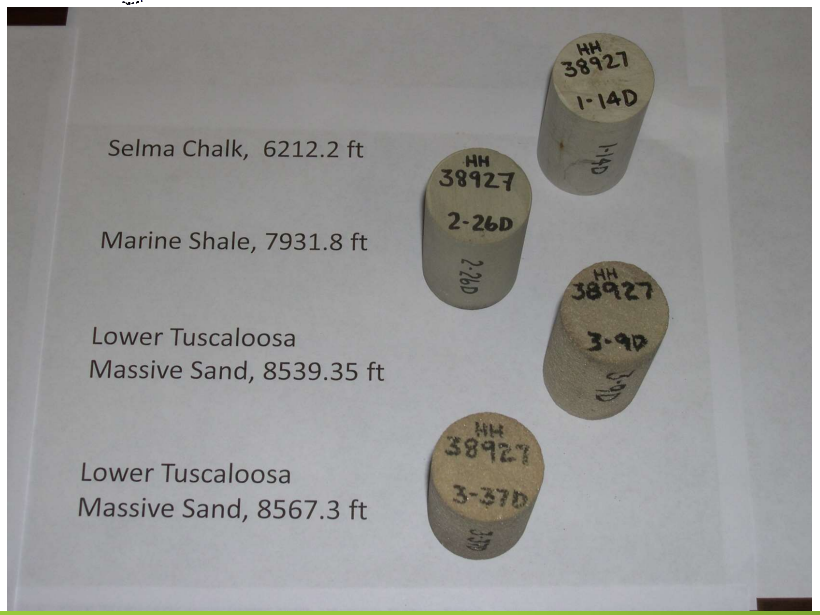

Experimental plan

NATIONAL ENERGY TECHNOLOGY LABORATORY

Goal : To understand the impacts of CO_2-brine-rock interactions on chemistry process, porosity, permeability properties on storage formations and seals.

Approach : To characterize physical and chemical attributes of formation rock and brine samples before and after the exposure of CO_2. To measure porosity, permeability, petrography, and mineralogy *via* various techniques, such as CT imaging, microscopy. Conducted three six-months of CO_2/brine/Massive sand, Marine shale and Selma Chalk sandstone exposure experiments under sequestration conditions (85 °C and 3,500 psi of CO_2).

No significant change in porosity and permeability (Selma Chalk)

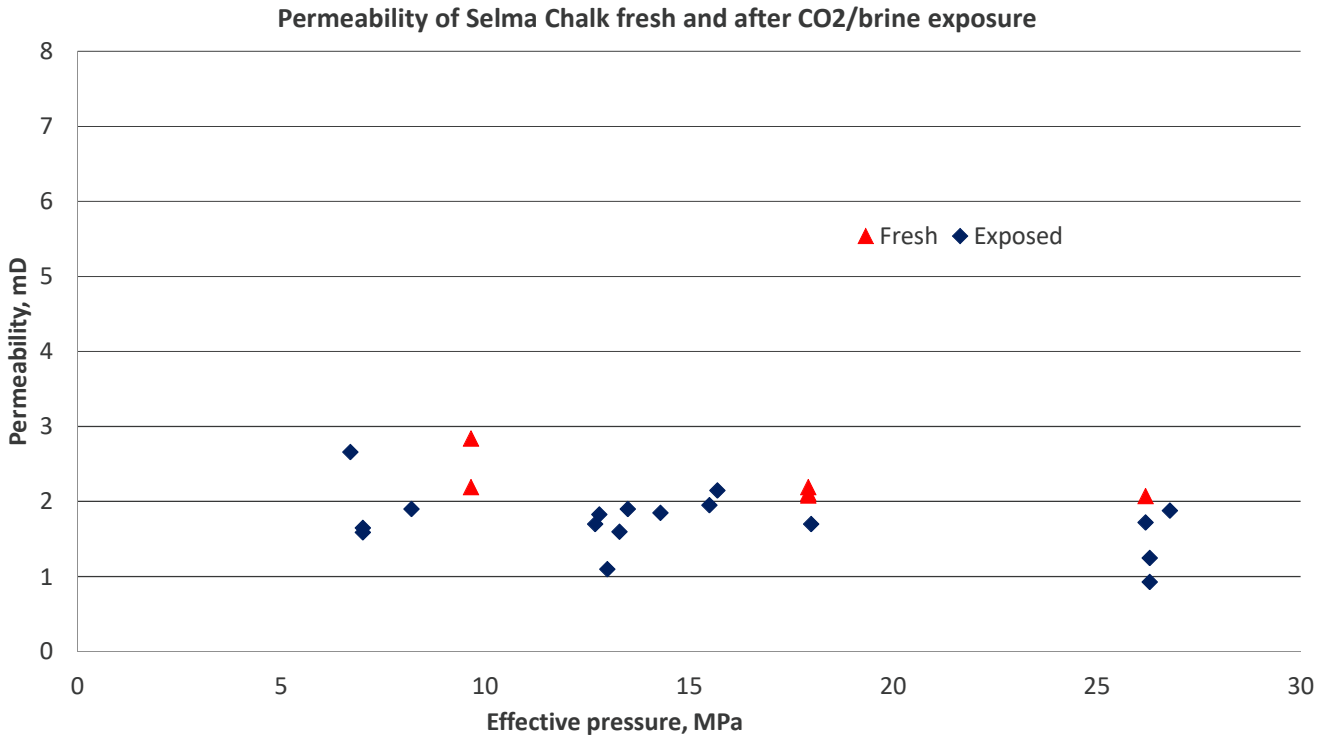

CT images of the Selma Chalk fresh (left) vs. exposed (right)

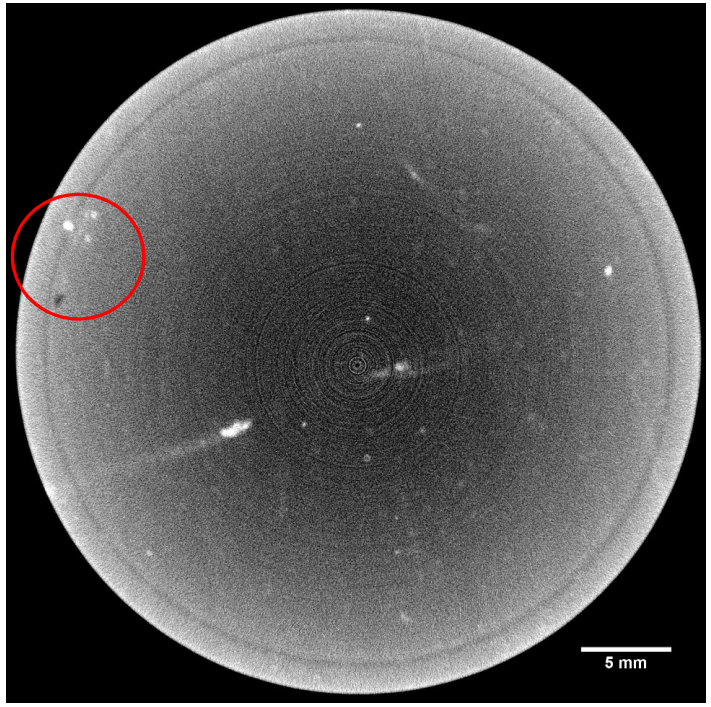

Fresh

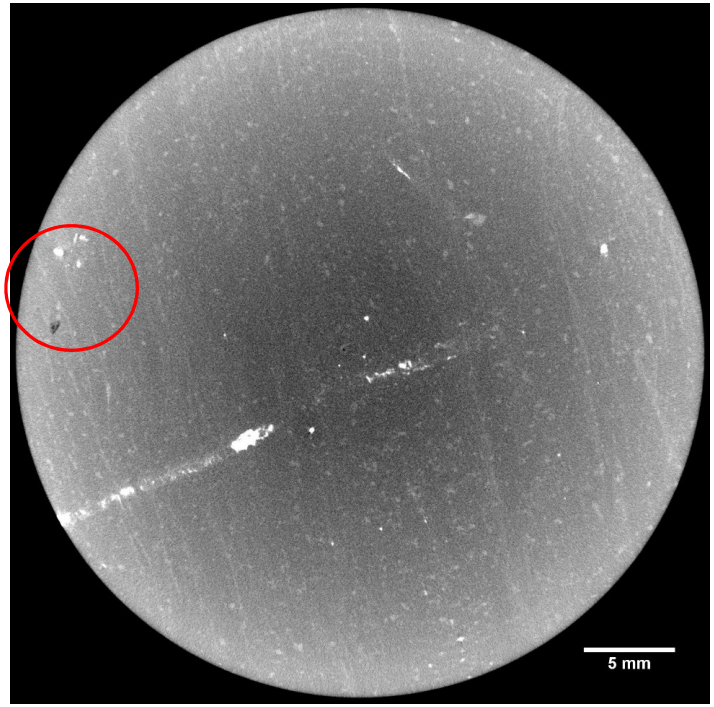

Exposed

SEM image of Selma Chalk fresh (left) vs. exposed (right)

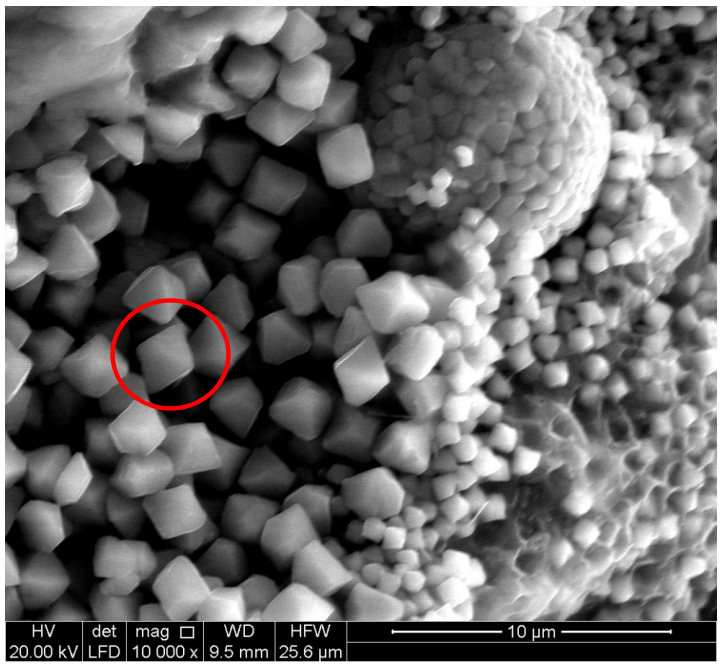

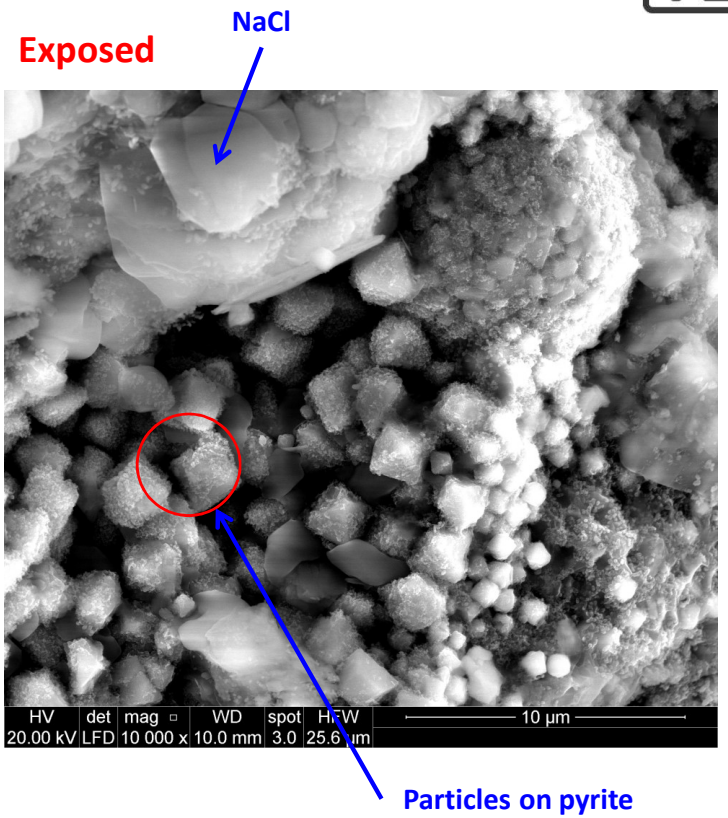

Changes observed: Mechanical loss of pyrite, NaCl residue,

Brine interacted with Selma Chalk/CO2 after 6 months

	Synthetic Lower Tuscaloosa Brine	Brine interacted with Selma chalk
	Ave. (ppm)	Ave. (ppm)
Al	1.06	0.74
B	1.89	6.90
Ba	9.55	4.25
Ca	11798	12404
Cd	0.03	0.03
Co	0.05	0.29
Cu	0.37	0.58
Fe	124	142
K	412	528
Mg	1035	1192
Mn	0.07	0.71
Na	43743	45946
Ni	0.73	2.70
Pb	<DL	193.48
S	166	320
Si	<DL	44.57
Sn	0.25	0.26
Sr	696	699
Chloride	92223	91959
Bromide	432	432.20
Nitrate	<QL	5.00
Sulfate	238	303

Summary for Selma Chalk results

- Increased conc. of Ca, Fe, K, Mg, Na, and Si in the reacted brine may suggest some dissolution of calcite (Selma Chalk)
- The permeability of Selma Chalk showed no significant change after 6 month in CO_2/brine at 85 C and 3500 psi. **(Good Seal)**

LT sandstone permeability and porosity reduced by 17% and 6.4%

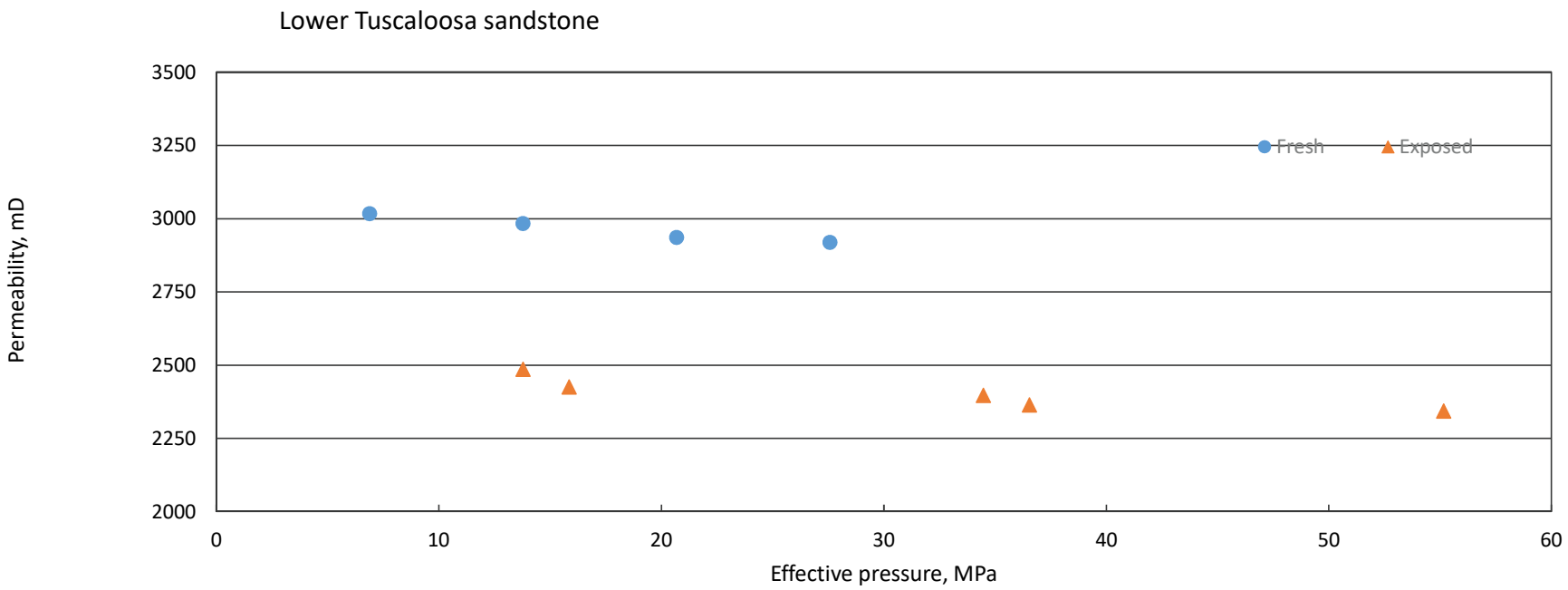

CT images of LT Massive Sand fresh (left) vs. exposed (right)

- Fresh

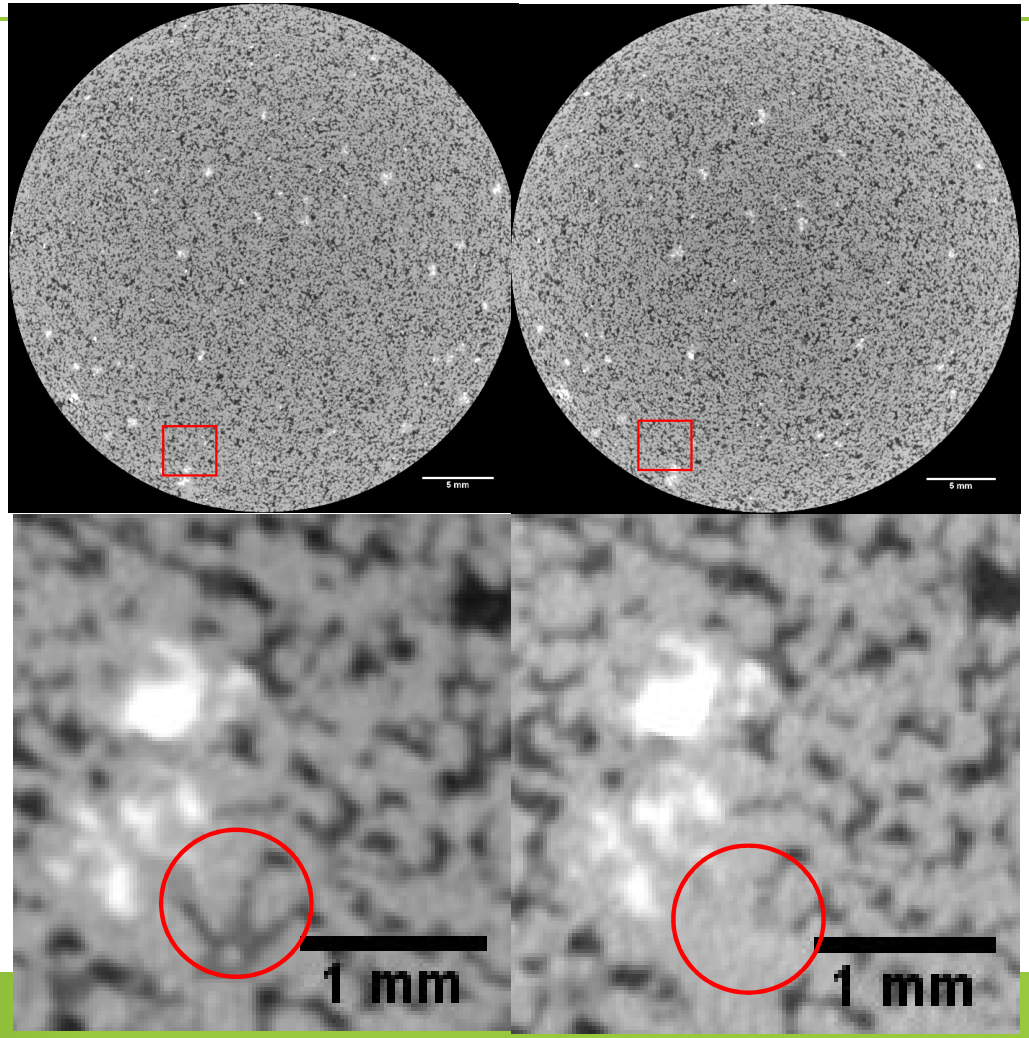

Exposed

CT images of LT Massive Sand fresh (left) vs. exposed (right)

- Fresh

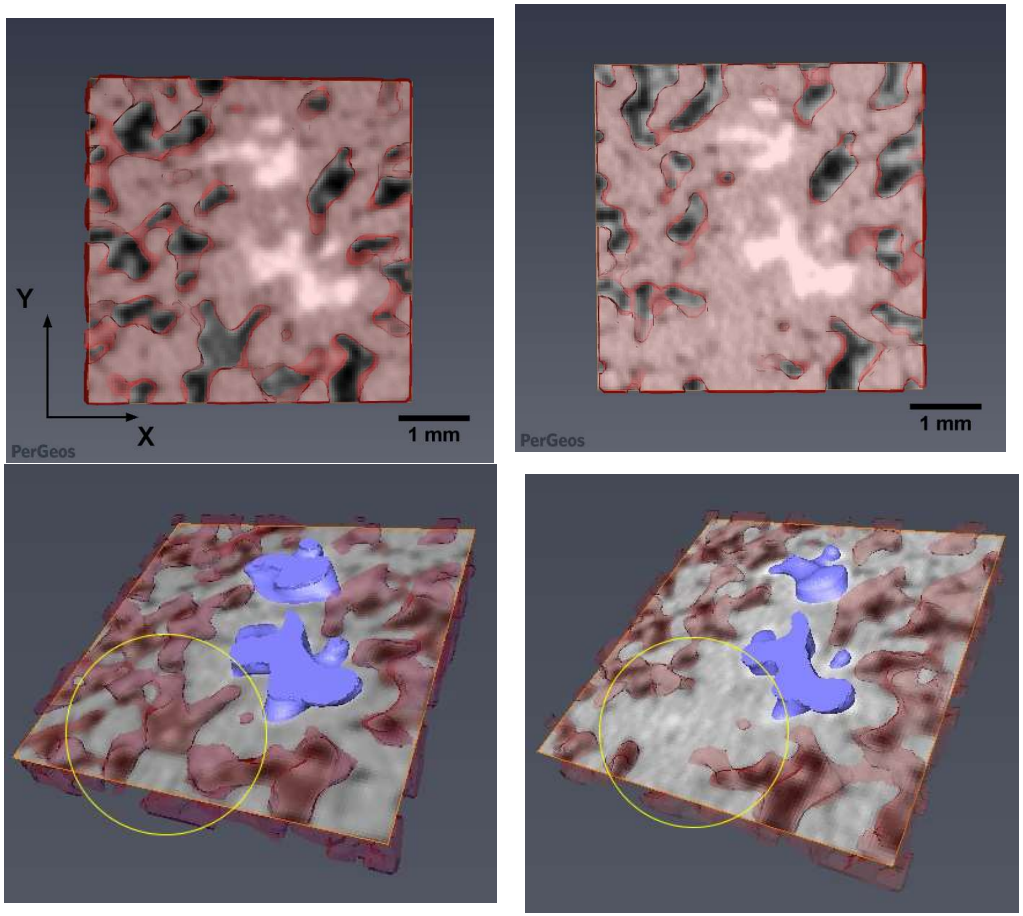

Exposed

SEM of LT Massive Sand fresh (left) vs. exposed (center), exposed rinsed with H2O (right)

NATIONAL ENERGY TECHNOLOGY LABORATORY

Fresh

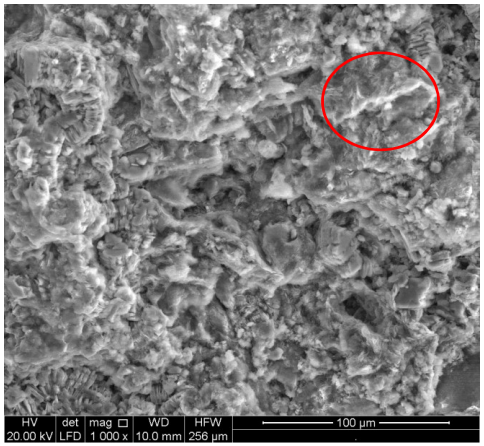

Exposed

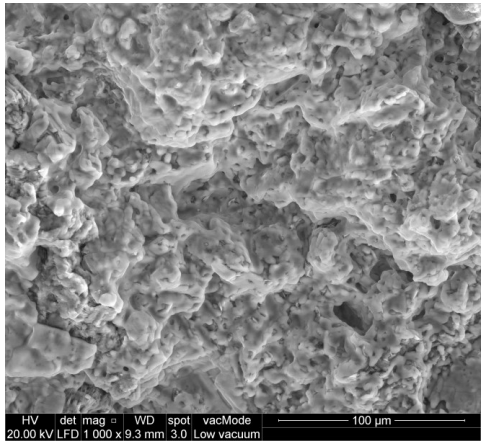

Exposed then DI H_2O rinsed

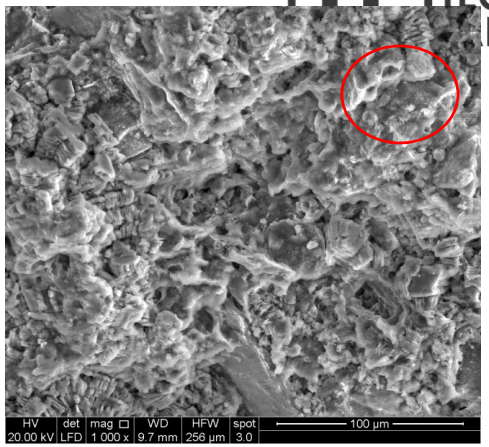

NaCl coating

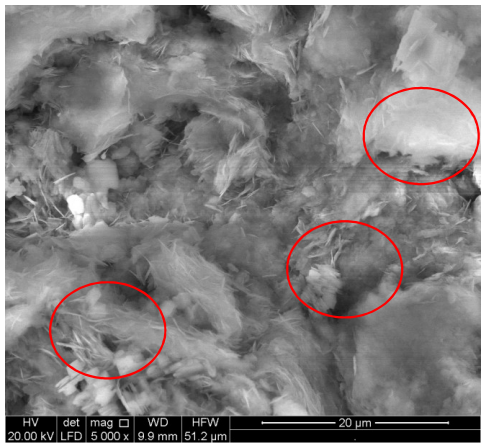

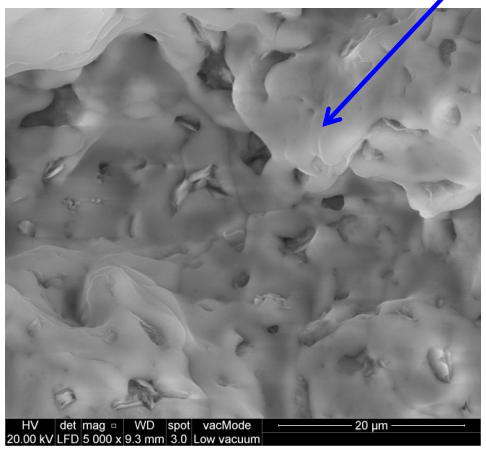

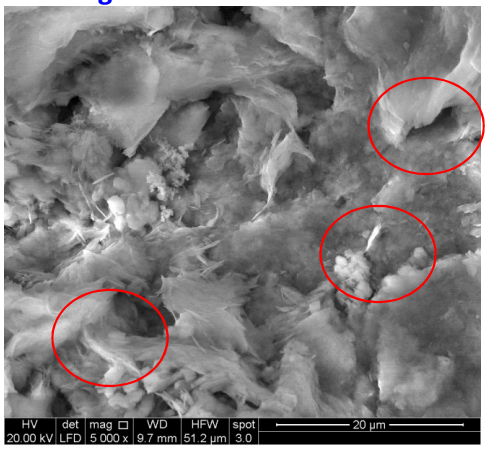

Brine interacted with LT Massive Sand/CO2 after 6 months

	Synthetic Lower Tuscaloosa, Brine batch # 3	Brine interacted with Lower Tuscaloosa Massive sand
	Ave. (ppm)	Ave. (ppm)
Al	~	2.5
Ba	9.3	6.9
Ca	10983	10743
Cr	0.13	0.6
Cu	~	3.2
Fe	128	176
K	374	372
Mg	999	1033
Mn	~	2.7
Na	41122	42555
Ni	0.6	3.4
Si	~	30.2
Sr	651	663
Chloride	87412	88230
Bromide	458	458
Sulfate	236	239

Summary for Lower Tuscaloosa sandstone results

- Increased conc. of Al, Ca, Fe, Mg, Na and Si in the reacted brine may suggest the dissolution of feldspar (Massive Sand)
- The permeability of Massive Sand decreased by 17% after 6 month in CO_2/brine at 85 C and 3500 psi. The observation may relate to mineral dissolution (feldspar,..) and precipitation (kaolinite,..).

Permeability fresh vs. exposed for Marine shale

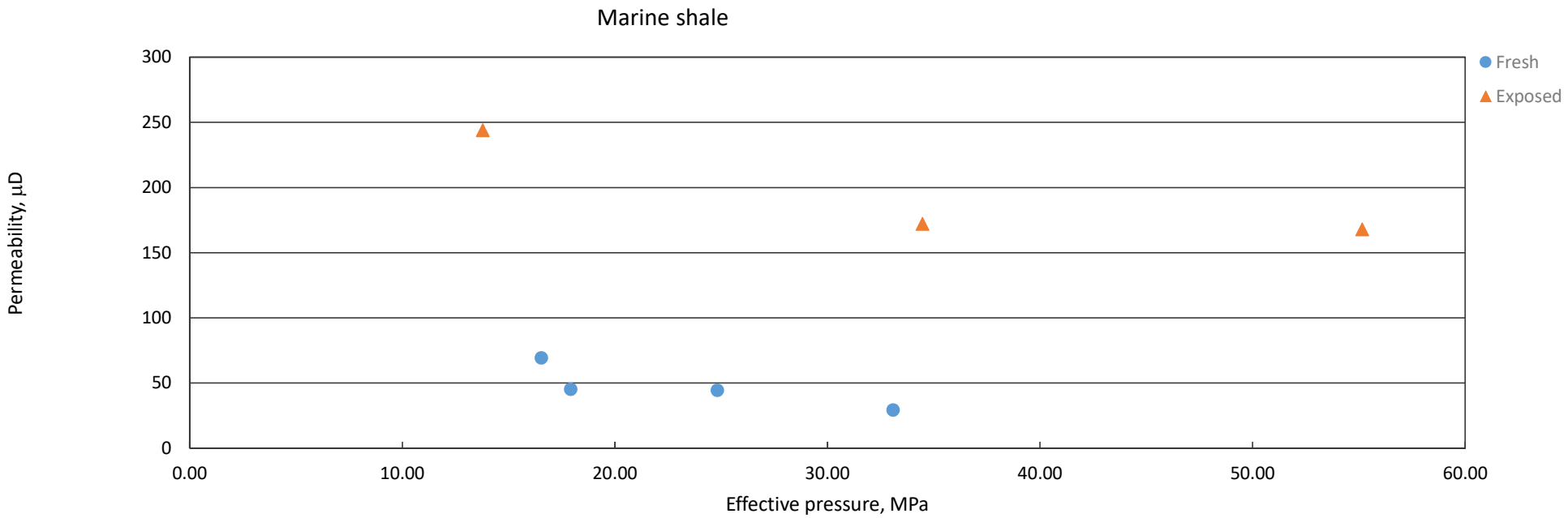

Porosity 8.65 to 8.56%

CT images of Marine shale fresh (left) vs. exposed (right)

Fresh

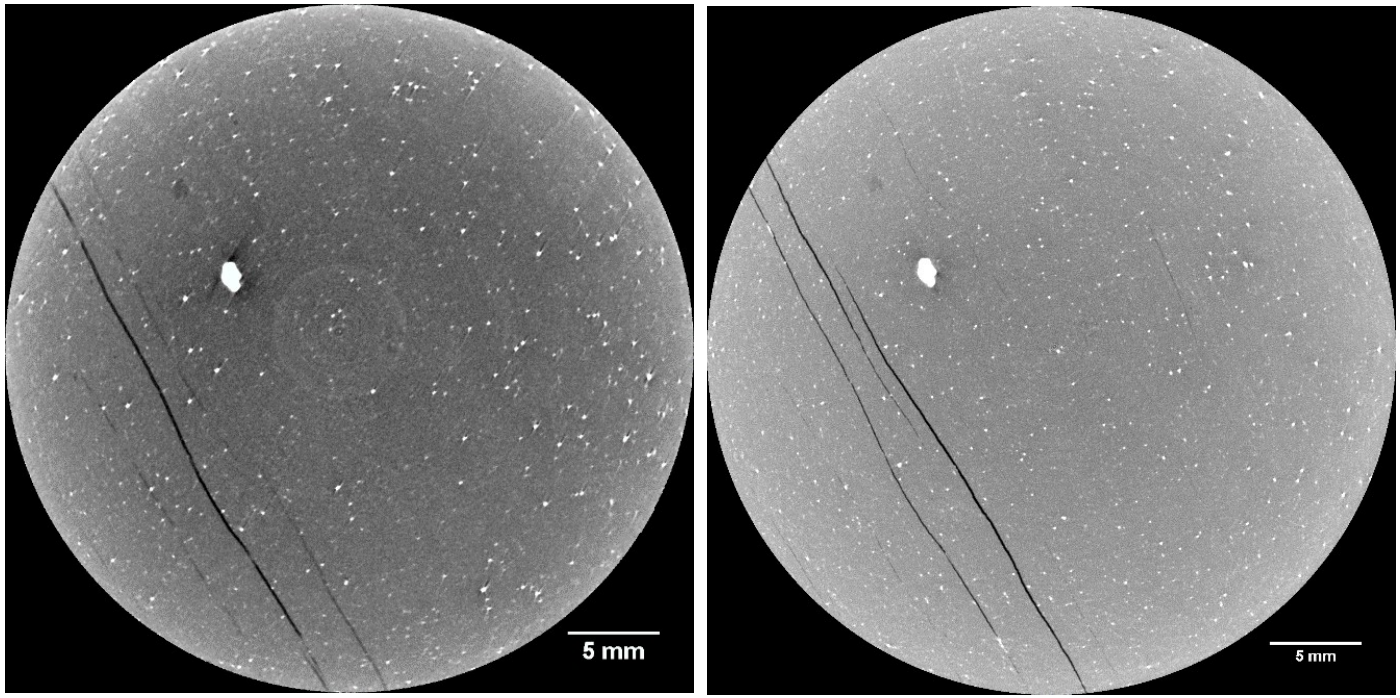

Exposed

CT images of Marine Shale fresh (top) vs. exposed (bottom)

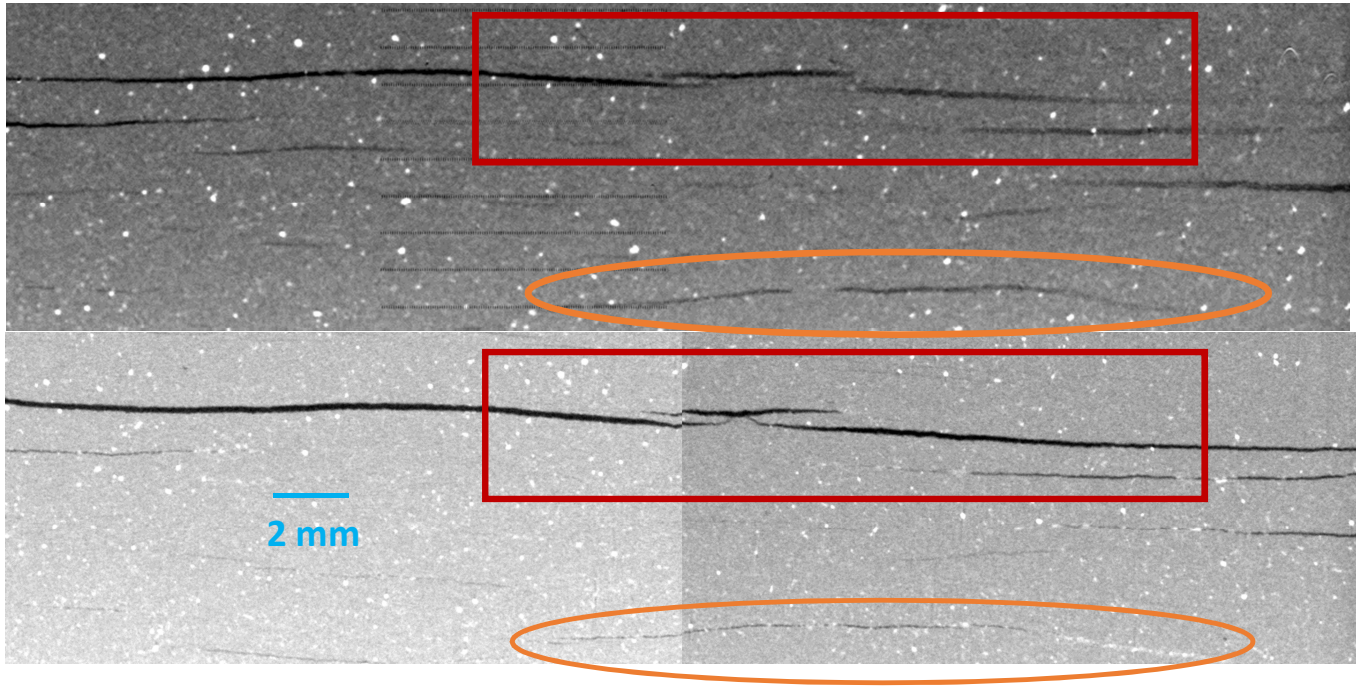

Brine interacted with Marine Shale/CO2 after 6 months

	Synthetic Lower Tuscaloosa Brine, batch # 4	Brine interacted with Marine Shale
	Ave. (ppm)	Ave. (ppm)
Al	1.13	~
Ba	9.48	2
Ca	11030	11392
Cr	0.133	1
Cu	~	~
Fe	128	205
K	373	340
Mg	1009	1081
Mn	~	7
Na	42063	43073
Ni	0.59	8
Si	~	35
Sr	661	565
Chloride	87524	87008
Bromide	459	459
Sulfate	235	389

Summary for Marine shale results

- Increased conc. of Ca, Fe, Mg, Na, and Si in the reacted brine may suggest some dissolution of kaolinite, illite, chlorite and calcite (Marine shale)
- The permeability of Marine shale increased by 3.4 times after 6 month in CO_2/brine at 85 C and 3500 psi. The observation may relate to mineral dissolution (feldspar,..), precipitation (kaolinite,..), delamination that resulted in creating more connection of fractures thus increase the permeability.

Summary of experimental study

- The permeability of LT Massive Sand decreased by 17% after 6 month in CO_2/brine at 85 C and 3500 psi. The observation may relate to mineral dissolution (feldspar,..) and precipitation (kaolinite,..).
- Some change in permeability of Marine shale after 6 month in CO_2/brine exposure due to creating more connective fractures.
- Selma chalk (seal) shows no observed changes in permeability/porosity after 6 months exposure in CO2/brine under CO2 storage conditions.
- Overall the Lower Tuscaloosa formation is a suitable location for CO2 storage from 6 months experimental study !
- Can we predict these results via computer simulation and extend the predictions beyond 6 months ?

Model to predict permeability/porosity after six month exposure under CO2/brine

Model domain and governing equations

1-D no flow reactive transport model

Software used: CrunchFlow

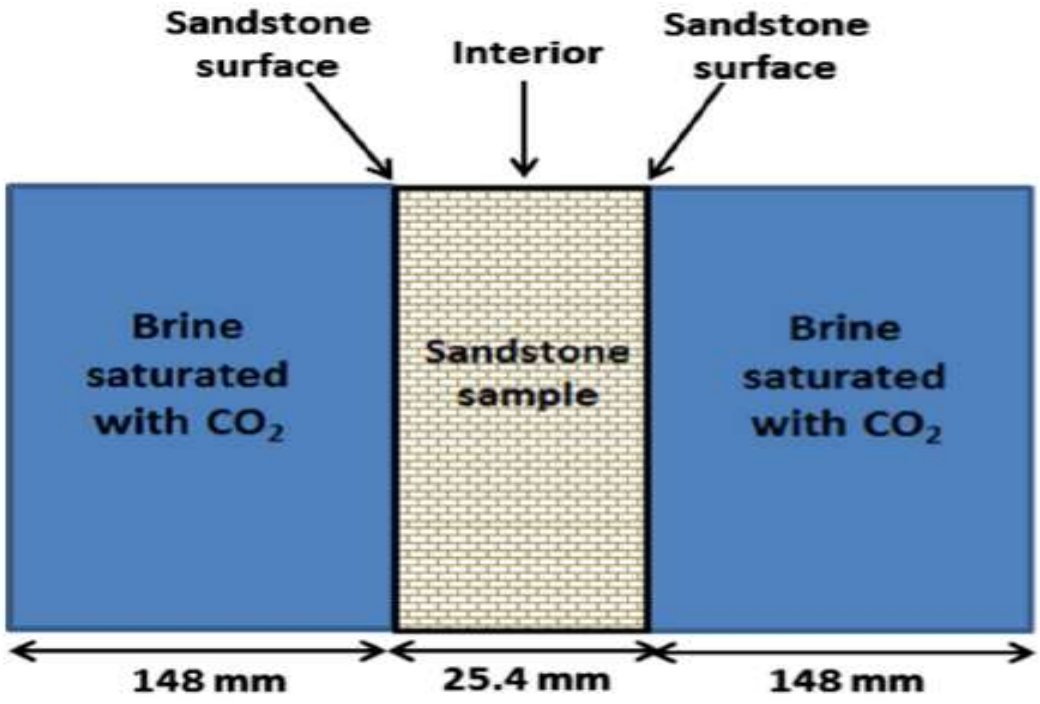

Mass conservation equation

$$\frac{d(\phi C_i)}{dt} = \frac{d}{dx}(\phi D_{ie}\frac{dC_i}{dx}) \pm \sum_{i=1}^{N} v_{ir}R_{ir}$$

Diffusion term Reaction term

Porosity evolution equation

$$\phi(t) = 1 - \sum_{i=1}^{m} fr_i(t) - fr_n$$

Rate of mineral dissolution/precipitation

$$R_{ir} = A\sum_{l=1}^{M} k_l \left(\prod_{i=1}^{N} a_i^{p_i}\right)\left(1 - \frac{Q}{K_{eq}}\right)$$

Effective diffusivity

$$D_e = D_0\phi^m$$

Model set-up

Mineral compositions of unreacted Lower Tuscaloosa and Selma Chalk samples

Mineral name	Volume percentage (%)—Lower Tuscaloosa sandstone	Volume percentage (%)—Selma Chalk
Chlorite ($Mg_{2.964}Fe_{1.927}Al_{2.483}Ca_{0.011}Si_{2.633}O_{10}(OH)_8$)	1.46	2.63
Microcline ($KAlSi_3O_8$)	0.73	0
Muscovite/Illite ($K_{0.85}Al_{2.85}Si_{3.15}O_{10}(OH)_2$)	0.73	1.75
Kaolinite ($Al_2Si_2O_5(OH)_4$)	0.73	1.75
Quartz (SiO_2)	68.1	2.63
Na-feldspar ($NaAlSi_3O_8$)	1.46	0
Calcite ($CaCO_3$)	0	78.8
Porosity	26.8	12.4
Total	100	100

Model set-up

Equilibrium constants (K_{eq}) and reaction rate constants (k)

Reaction	Equilibrium Constant at 85°C (K_{eq})	Rate Coefficient at 85°C, k, (mol/(m²s)[a]	Value of $\prod_{i=1}^{N} a_i^{p_i}$
quartz dissolution/precipitation (85 °C) $SiO_2 + 2H_2O \leftrightarrow H_4SiO_4(aq)$	$10^{-1.81}$	$10^{-11.38}$	1.0
SiO_2 (am) dissolution/precipitation (85 °C) $SiO_2(am) + 2H_2O \leftrightarrow H_4SiO_4(aq)$	$10^{-2.84}$	$10^{-7.09}$	1.0
Na-rich feldspar dissolution/precipitation (85 °C) $NaAlSi_3O_8 + 4H^+ + 4H_2O \leftrightarrow Na^+ + Al^{3+} + 3H_4SiO_4(aq)$	$10^{-0.64}$	For pH-independent dissolution/ precipitation, $k_1 = 10^{-11.29}$; For pH-dependent dissolution, $k_2 = 10^{-8.54}$.	For pH-independent dissolution/ precipitation, $\prod_{i=1}^{N} a_i^{p_i} = 1.0$; For pH-dependent dissolution, $\prod_{i=1}^{N} a_i^{p_i} = [H^+]^{0.5}$
Ca-rich feldspar dissolution/precipitation (85 °C) $CaAl_2Si_2O_8 + 8H^+ \leftrightarrow Ca^{2+} + 2Al^{3+} + 2H_4SiO_4(aq)$	$10^{16.53}$	For pH-independent dissolution/ precipitation, $k_1 = 10^{-11.29}$; For pH-dependent dissolution, $k_2 = 10^{-8.54}$.	For pH-independent dissolution/ precipitation, $\prod_{i=1}^{N} a_i^{p_i} = 1.0$; For pH-dependent dissolution, $\prod_{i=1}^{N} a_i^{p_i} = [H^+]^{0.5}$

$$R_{ir} = A \sum_{l=1}^{M} k_l \left(\prod_{i=1}^{N} a_i^{p_i} \right) \left(1 - \frac{Q}{K_{eq}} \right)$$

Reaction	Equilibrium Constant at 85°C (K_{eq})	Rate Coefficient at 85°C, k, (mol/(m^{2}s)[a]	Value of $\prod_{i=1}^{N} a_i^{p_i}$
microcline dissolution/precipitation (85 °C) $KAlSi_3O_8 + 4H^+ + 4H_2O \leftrightarrow K^+ + Al^{3+} + 3H_4SiO_4(aq)$	$10^{-1.58}$	For pH-independent dissolution/ precipitation, $k_1 = 10^{-11.29}$; For pH-dependent dissolution, $k_2 = 10^{-8.54}$.	For pH-independent dissolution/ precipitation, $\prod_{i=1}^{N} a_i^{p_i} = 1.0$; For pH-dependent dissolution, $\prod_{i=1}^{N} a_i^{p_i} = [H^+]^{0.5}$
Ba-bearing feldspar dissolution/precipitation (85 °C) $BaAl_2Si_2O_8 + 8H^+ \leftrightarrow Ba^{2+} + 2Al^{3+} + 2H_4SiO_4(aq)$	$10^{16.53}$	For pH-independent dissolution/ precipitation, $k_1 = 10^{-11.29}$; For pH-dependent dissolution, $k_2 = 10^{-8.54}$.	For pH-independent dissolution/ precipitation, $\prod_{i=1}^{N} a_i^{p_i} = 1.0$; For pH-dependent dissolution, $\prod_{i=1}^{N} a_i^{p_i} = [H^+]^{0.5}$
annite dissolution/precipitation (85 °C) $KFe_3AlSi_3O_{10}(OH)_2 + 10H^+ \leftrightarrow Al^{3+} + 3Fe^{2+} + K^+ + 3H_4SiO_4(aq)$	$10^{20.83}$	For pH-independent dissolution/ precipitation, $k_1 = 10^{-11.49}$; For pH-dependent dissolution, $k_2 = 10^{-8.49}$	For reaction (1), $\prod_{i=1}^{N} a_i^{p_i} = 1.0$; For reaction (2), $\prod_{i=1}^{N} a_i^{p_i} = [H^+]^{0.53}$

kaolinite dissolution/precipitation (85 °C) $Al_2Si_2O_5(OH)_4+6H^+ \leftrightarrow 2Al^{3+}+H_2O+2H_4SiO_4(aq)$	**$10^{1.56}$ [b]**	**For dissolution, k =$10^{-10.10}$; for precipitation, k = $10^{-12.15}$**	**For dissolution, $\prod_{i=1}^{N} a_i^{p_i} = [H^+]^{0.4}$; for precipitation, $\prod_{i=1}^{N} a_i^{p_i} = [Al^{3+}]$**
barite dissolution/precipitation (85 °C) $BaSO_4 \leftrightarrow Ba^{2+}+SO_4^{2-}$	$10^{-9.61}$	$10^{2.97}$	$[Ba^{2+}][SO_4^{2-}]$
gypsum dissolution/precipitation (85 °C) $CaSO_4 \cdot 2H_2O \leftrightarrow Ca^{2+}+SO_4^{2-}+2H_2O$	$10^{-4.885}$	$10^{-4.16}$	1.0
siderite dissolution/precipitation (85 °C) $FeCO_3+H^+ \leftrightarrow Fe^{2+}+HCO_3^-$	$10^{-1.20}$	$10^{-7.7}$	$[HCO_3^-]$
muscovite/illite dissolution/precipitation (85 °C) $KAl_3Si_3O_{10}(OH)_2+10H^+ \leftrightarrow 3Al^{3+}+K^++3H_4SiO_4(aq)$	$10^{5.96}$	$10^{-10.33}$	1.0
dolomite dissolution/precipitation (85 °C) $CaMg(CO_3)_2+2H^+ \leftrightarrow Ca^{2+}+Mg^{2+}+2HCO_3^-$	$10^{1.425}$	$10^{-14.43}$	1.0
calcite dissolution/precipitation (85 °C) $CaCO_3+H^+ \leftrightarrow Ca^{2+}+HCO_3^-$	$10^{0.68}$	For dissolution, k =$10^{-2.01}$; for precipitation, k = $10^{-7.31}$	For dissolution, $\prod_{i=1}^{N} a_i^{p_i} = [H^+]$; for precipitation, $\prod_{i=1}^{N} a_i^{p_i} = [Ca^{2+}][HCO_3^-]$

Permeability calculation

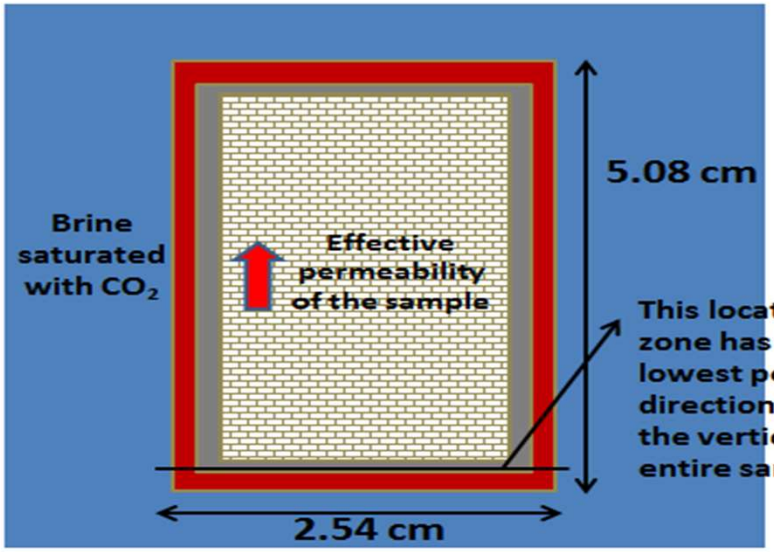

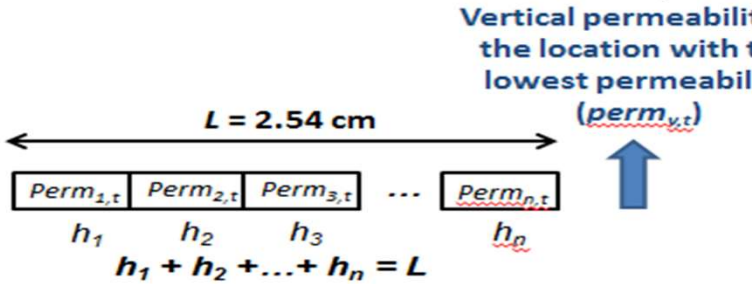

$$perm_{v,t} = \frac{\sum_{i=1}^{n} h_i perm_{i,t}}{L}$$

Calculation of $perm_{i,t}$ (Kumpel, 2003):

$$\frac{perm_{i,t}}{perm_{i,0}} = \left(\frac{\emptyset_{i,t}}{\emptyset_{i,0}}\right)^{n}$$

Porosity and mineral composition change—Lower Tuscaloosa sandstone

Mineral name	Volume percentage (%, before reaction with brine and CO_2)	Specific surface area (m^2/g)	Molar volume (cm^3/mol)
Mineral compositions of unreacted Lower Tuscaloosa sandstone			
Chlorite[a] $(Mg_{2.964}Fe_{1.927}Al_{2.483}Ca_{0.011}Si_{2.633}O_{10}(OH)_8)$	1.464	5.06	210.3
Microcline ($KAlSi_3O_8$)[b]	0.732	0.39	100.4
Muscovite/Illite ($K_{0.85}Al_{2.85}Si_{3.15}O_{10}(OH)_2$)[c]	0.732	3.40	144.5
Kaolinite ($Al_2Si_2O_5(OH)_4$)[d]	0.732	15.0	99.3
Na-feldspar[e] ($NaAlSi_3O_8$)	1.464	0.39	100.4
Quartz (SiO_2)[f]	68.08	0.10	22.7
Porosity	26.80	--	--

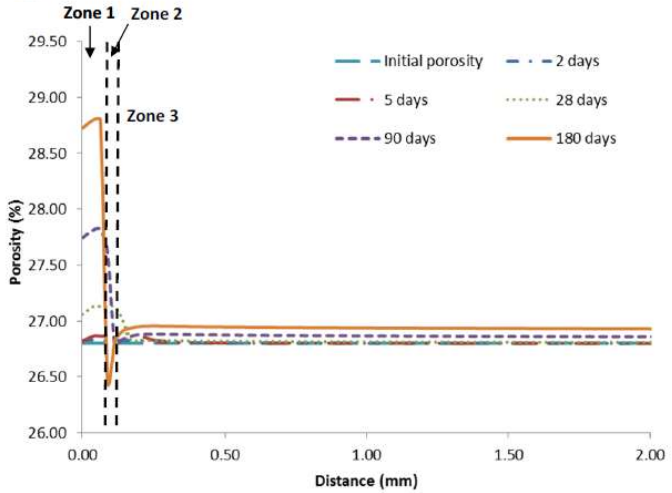

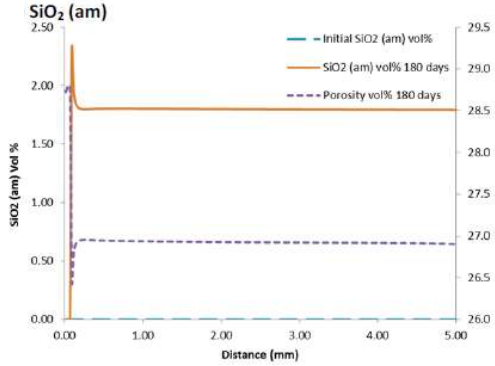

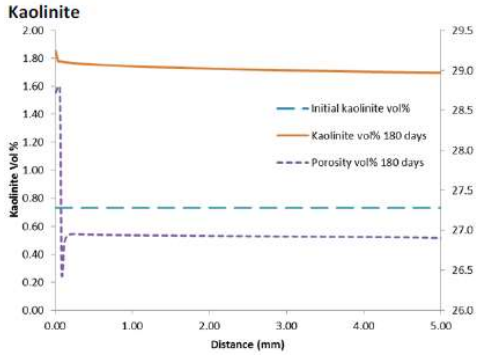

Solution chemistry and permeability change—180 days (Lower Tuscaloosa)

Element/ component	Lower Tuscaloosa	
	Measured concentration (mg/kg water)	Model-predicted concentration (mg/kg water)
Ca	13,201	11,829
Na	48,387	43,946
Mg	1,240	1,130
K	530.0	576.8
Fe	210.0	137.9
Si	22.90	9.743
Al	2.200	97.77
Ba	5.900	0.160
Dissolved CO_2	Not measured	29,546

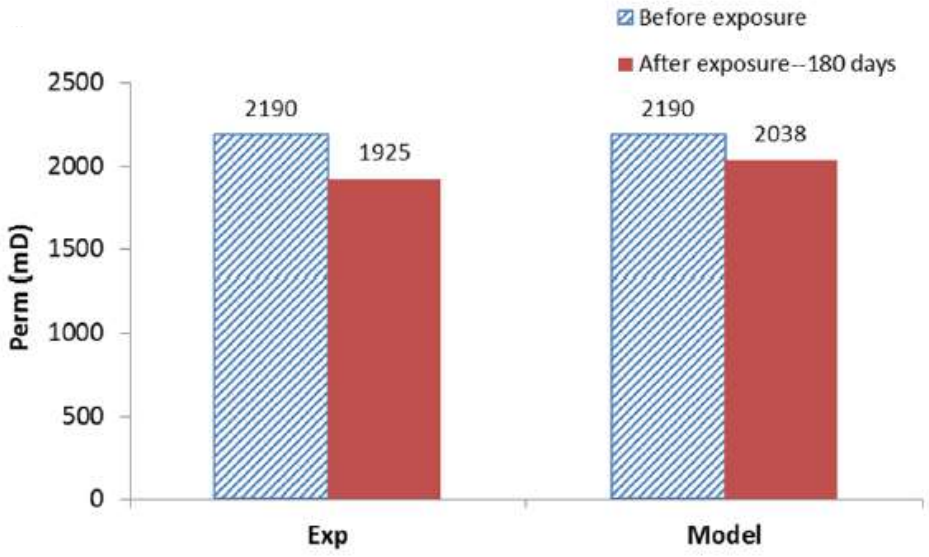

$$\frac{perm_{i,t}}{perm_{i,0}} = \left(\frac{\emptyset_{i,t}}{\emptyset_{i,0}}\right)^{6.0}$$

LT Massive Sandstone permeability vs. time

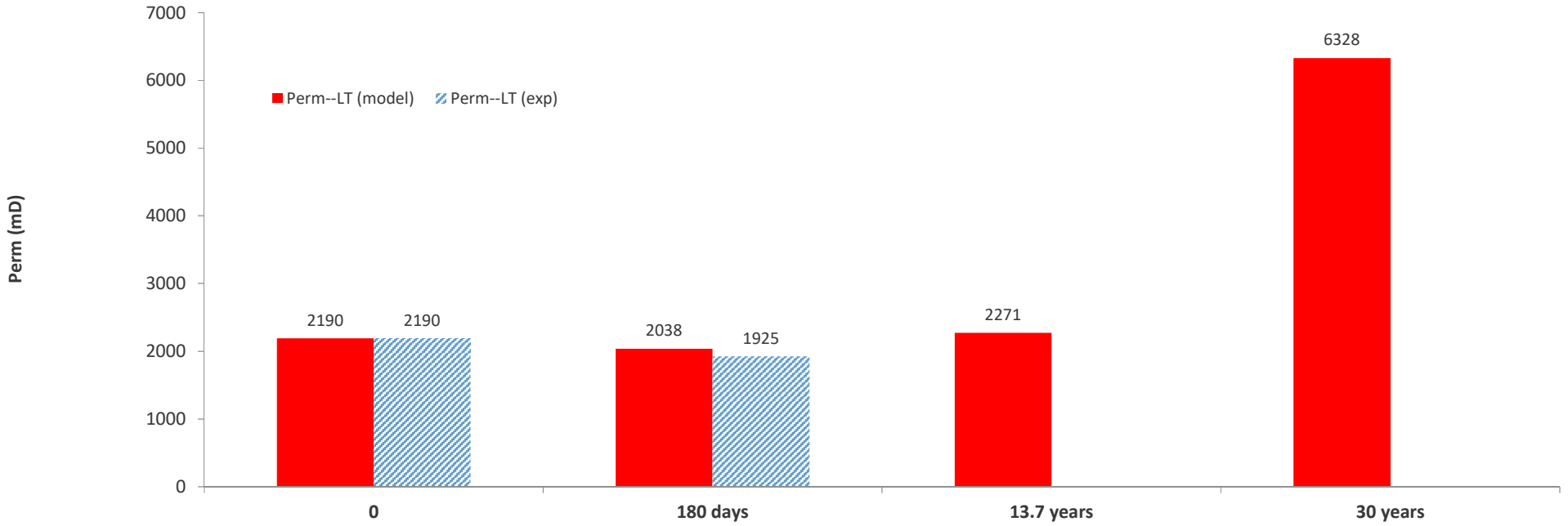

Porosity and mineral composition change—Selma Chalk

Mineral name	Volume percentage (%, before reaction with brine and CO_2)	Specific surface area (m^2/g)	Molar volume (cm^3/mol)
Mineral compositions of unreacted Selma Chalk			
Calcite $(CaCO_3)^g$	78.84	1.00	36.9
Chlorite $(Mg_{2.964}Fe_{1.927}Al_{2.483}Ca_{0.011}Si_{2.633}O_{10}(OH)_8)$	2.630	5.06	210.3
Muscovite/Illite $(K_{0.85}Al_{2.85}Si_{3.15}O_{10}(OH)_2)$	1.752	3.40	144.5
Kaolinite $(Al_2Si_2O_5(OH)_4)$	1.752	15.0	99.3
Quartz (SiO_2)	2.630	0.10	22.7
Porosity	12.40	--	--

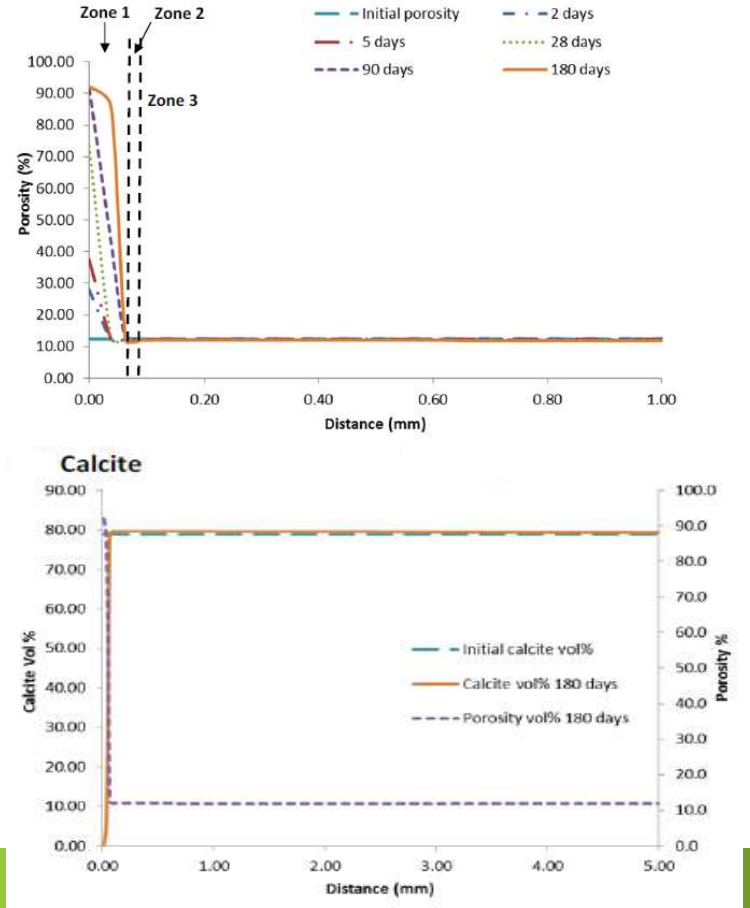

Solution chemistry and permeability change—180 days (Selma Chalk)

Element/ component	Selma Chalk	
	Measured concentration (mg/kg water)	Model-predicted concentration (mg/kg water)
Ca	12,404	11,596
Na	45,946	43,748
Mg	1,192	1,214
K	528.0	767.2
Fe	142.0	120.0
Si	44.57	8.067
Al	0.740	76.41
Ba	4.250	0.160
Dissolved CO_2	Not measured	29,602

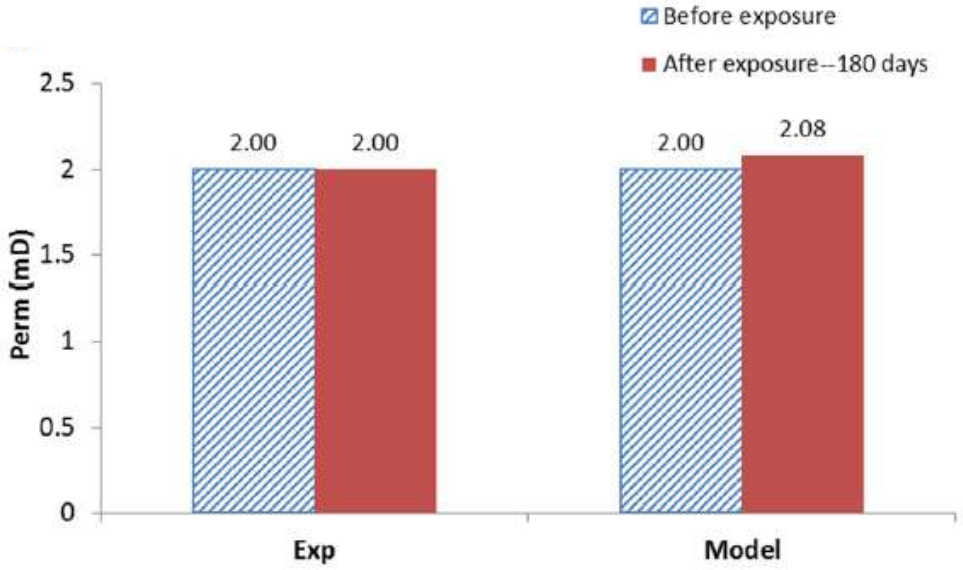

$$\frac{perm_{i,t}}{perm_{i,o}} = \left(\frac{\emptyset_{i,t}}{\emptyset_{i,o}}\right)^{1.7}$$

Selma Chalk permeability vs. time

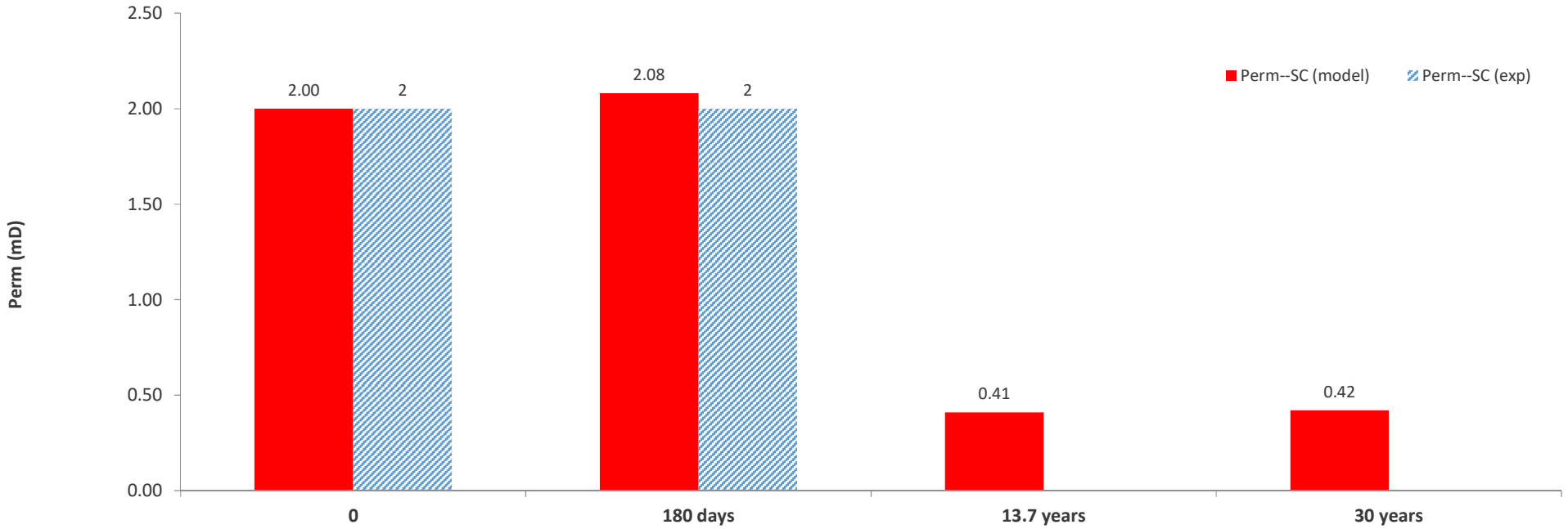

Summary of simulation

- LT sandstone : Measured permeability decrease—2190 mD to 1925 mD; model- predicted permeability decrease —2190 mD to 2038 mD. Selma chalk : predicted 2.08 mD cs that of 2 mD experimental observation (6 months)
- The model predicts the permeability of sandstone will increase from 2,190 to 6,328 mD after 30 years
- The model also predicts the permeability of Selma chalk (seal) will decrease from 2 to 0.42 mD after 30 years.
- The prediction of changes of the reservoir rock and the sealing formation rock after 30 years exposure implies potential for safe containment of injected CO_2.

Relate to CO_2 sequestration

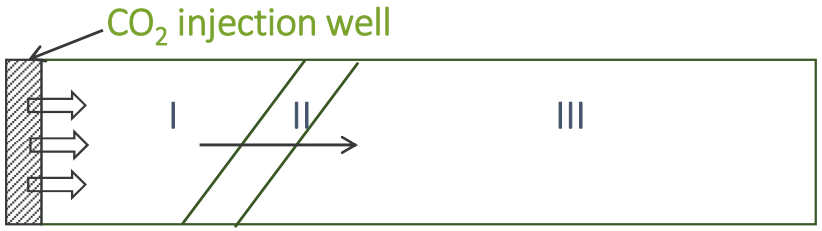

Zone I: CO_2 plume
Zone II: Brine rich in CO_2

During the CO_2 injection period, Zone II is pushed away by continuous injection of CO_2 and does not reside in a location for long enough time to cause permeability reduction of that location.

Chemical reactions have less impact during the CO_2 injection stage

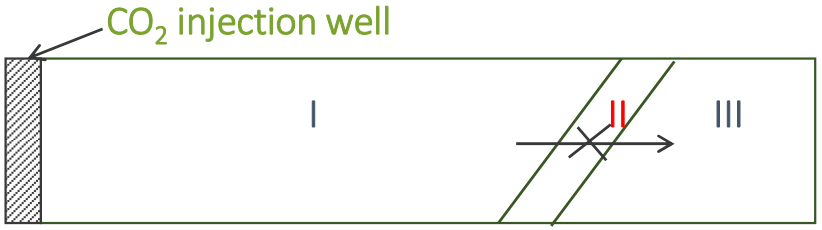

After termination of CO_2 injection, Zone II will reside in a certain location for long enough time to cause permeability change of that location, which serves as a barrier to mitigate migration of CO_2.

Results and discussion

Limitations of the core-scale model

- Good for static system with no flow through fractures
- Results valid for homogeneous samples
- A separate model needs to be developed for a flow-through system with fractured core samples.

Future work

Extending the core-scale results to field scale

Permeability evolution of core sample ≠ permeability evolution in the field

- A field scale model is developed using TOUGHREACT to investigate porosity and permeability change in a hypothetical CO_2 storage reservoir
- Important modeling parameters from the core-scale model are the basis to develop the field scale model

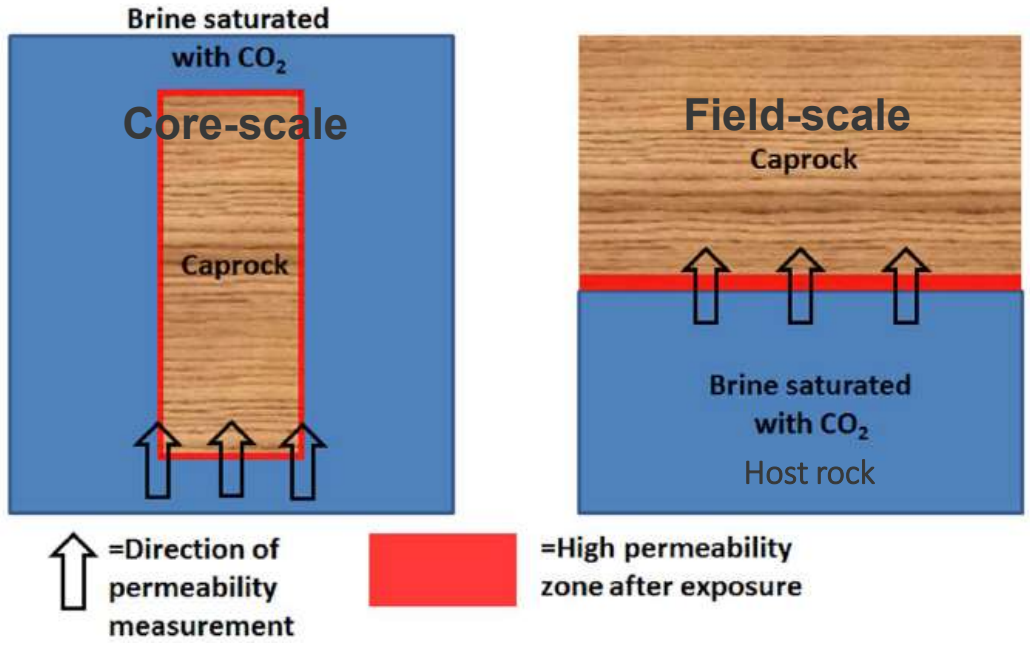


NATIONAL
ENERGY
TECHNOLOGY
LABORATORY
Thank you for your time!